Solid Freeform Fabrication 2022: Proceedings of the 33rd Annual International Solid Freeform Fabrication Symposium – An Additive Manufacturing Conference
Reviewed Paper

FEASIBILITY STUDY OF LARGE-SIZED ALUMINUM FACADES BY USING WIRE ARC ADDITIVE MANUFACTURING

Y. Yamagata*, T.Sagawa*, M.Nitawaki*, and T.Abe †

*Institute of Technology, Shimizu Corporation, Japan
† Graduate School of Science and Engineering, Saitama University, Japan

Abstract

Over the past few years, there has been growing interest in the fabrication of construction components by using wire arc additive manufacturing (WAAM). We focused on the finishing materials as a potential application for WAAM and began to consider fabricating aluminum building facades. However, there are several issues, such as fabrication size of 4-5m, aesthetics, and structural performance. Therefore, a trial fabrication and a non-destructive static loading test were conducted. In the study, an aluminum chair was used as a model because it contains the engineering basis of the building facades. In the trial fabrication, a method of leveling the build surface for each of the multiple layers was found to be effective for large-sized fabrication. Bead blasting was also effective in removing oxides from aluminum surfaces and adjusting the appearance. In the loading test, both displacement and strain measurements agreed well with the FEM analytical values. The results showed that WAAM has the possibility of fabricating large-sized aluminum building facades with the structural performance expected in the FEM analysis.

1. Introduction

The computation-based approach in design, called computational design, has been developed over the last decade [1] and is becoming more common among architects and designers. This method is used to derive the optimum shape through repeated trials in the program. However, the optimum shape may not be bound by existing concepts and be too complex to be realized by conventional manufacturing processes, such as machining or casting. For this reason, additive manufacturing (AM), which offers a high degree of freedom in modeling, has been attracting attention in the construction industry in recent years [2]. AM is defined as "process of joining materials to make parts from 3D model data, usually layer upon layer, as opposed to subtractive manufacturing and formative manufacturing methodologies" in the international standard ISO/ASTM52900:2021 [3]. AM can produce complex or customized parts directly from digital models. Therefore, products can be manufactured in one step as designed without the constraints of conventional manufacturing processes.

Regarding metal additive manufacturing, powder bed fusion (PBF) has been widely used for relatively high accuracy and high unit cost parts used in the automotive, aerospace, and medical industry [4]. In contrast, PBF has a limited range of applications in the construction industry. That is because construction components require a large size and low unit cost, whereas PBF has a relatively small build volume and high material and equipment costs. Thus, the use of directed energy deposition (DED) is being considered [5], which has a larger build volume and lower cost than PBF [6]. Especially, wire arc additive manufacturing (WAAM) is attracting attention among DED methods. WAAM is a method to form a target shape by layering weld beads using arc welding technology. Although WAAM is less accurate than other DED methods, it is superior in terms of build volume, cost, or mechanical properties [7], which has a high affinity with the construction industry. Recently, studies on the use of WAAM in the construction industry have been mainly focused on the fabrication of structural materials using steel [8][9]. However, there have been few studies on finishing materials using aluminum alloys, which are frequently used for building facades. Therefore, the purpose of this study was to investigate the feasibility of fabricating large-sized aluminum building facades by using WAAM.

There were several issues in using WAAM for fabricating building facades. Since aluminum alloys have a lower melting point and higher thermal conductivity than steel, the accuracy of the bead shape is prone to be lower due to temperature change during the deposition. This makes layer height variation from place to place and

makes it difficult to continue deposition when the height in the building direction becomes high. Furthermore, aluminum alloys are more prone to occur oxidation than steel [10], and the components fabricated by WAAM leave an uneven surface. This may negatively affect their aesthetics and structural performance. Therefore, these issues were studied by using a chair as a model, which requires both an aesthetically pleasing appearance and structural performance that can withstand realistic use. For the study, a trial fabrication and a non-destructive static loading test were conducted. In the trial fabrication, a method of leveling the build surface for each of the multiple layers was adopted and evaluated to increase the stackable height. The appearance of the chair was also checked immediately after deposition and after surface treatment by bead blasting to confirm the aesthetics. In the loading test, measured displacement and strain were compared with the FEM analysis results to evaluate the structural performance.

2. Design and FEM analysis

A chair was designed as a simple model that includes the engineering basis of building facades. The chair size was 420mm (width)×400mm (depth)×600mm (height) with a hollow cross-sectional structure, as shown in Figure 1. The uniform cross-sectional plate (5.0 mm width) and joints (8.0 mm width) were designed, and the joints structurally united the two plates on the front and back sides. The chair material was Al-5356, which is widely used for welding.

FEM analysis was performed for the preliminary evaluation of the structural performance. Table 1 shows the material properties of Al-5356 used in the analysis. The values were the nominal value of density [11] and the results of tensile tests on Al-5356 specimens fabricated by using WAAM [12][13]. The analysis was performed under the condition that a static load of 981N was applied to the seat surface. Figure 2 shows the FEM analysis results. The maximum total displacement was 29.9 mm near the top of the chair, as shown in Figure 2 (a). The maximum Mises stress was 80.4 MPa, and the stress was concentrated at the joints in the chair leg, as shown in Figure 2(b). The safety factor based on yield strength was 1.43, confirming that the chair was in the elastic range when a static load of 981N was applied.

Table 1 Material properties of Al-5356 used in the FEM analysis

Parameters	Unit	Value	Reference
Density	kg/m^3	2640	[11]
Young's modulus	GPa	68.4	[12]
Poisson's ratio	-	0.335	[12]
Yield strength	MPa	115	[13]

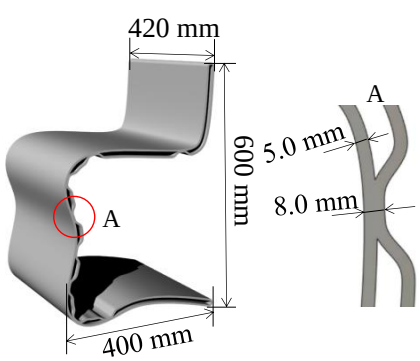

Fig.1 Chair design

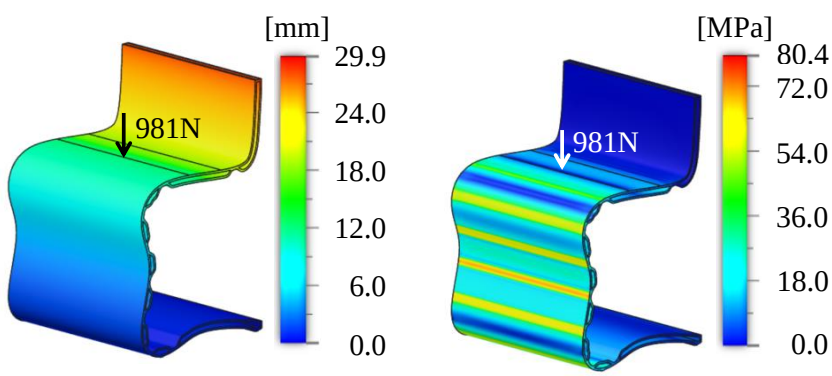

(a) Total displacement (b) Von Mises stress

Fig.2 FEM analysis results

3. Trial Fabrication

3.1 Fabrication procedure

To increase the stackable height, the method of leveling the build surface for each of the multiple layers was adopted. The leveling process was presumed to allow the deposition process to continue because the unevenness of the build surface would be removed. Figure 3 shows the schematic process sequence for the chair fabrication. Deposition of six layers, leveling the build surface with a grinding tool, measurement of the topmost bead width with calipers, and waiting for cooling were repeated. The deposition process was performed by robot-assisted welding. A Fronius CMT welding power source (TPS400i) combined with a Yaskawa Electric 6-DOF robot arm (MOTOMAN-AR1440) was used, as shown in Figure 4. Figure 5 shows the torch path for deposition. Since the deposited shapes were the same in all layers, the torch direction was always oriented vertically. The x and y coordinates of the starting point of the torch path were the same, and the torch travel direction alternated between counterclockwise and clockwise for each layer. Table 2 shows the welding parameters for deposition. A substrate made of A5052 with dimensions of 1000 mm × 650 mm × 5 mm was clamped on a lattice table, and the welding beads were deposited on it. The leveling process and measurement process were performed by human hands. The cooling process was performed by leaving the product at room temperature.

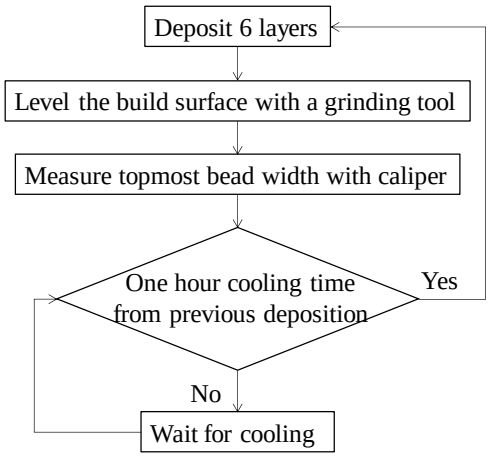

Fig.3 Process sequence for fabrication

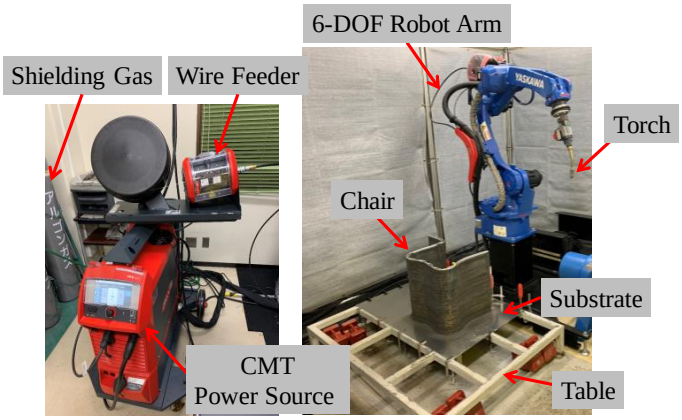

Fig.4 Setup for robot-assisted wire arc additive manufacturing

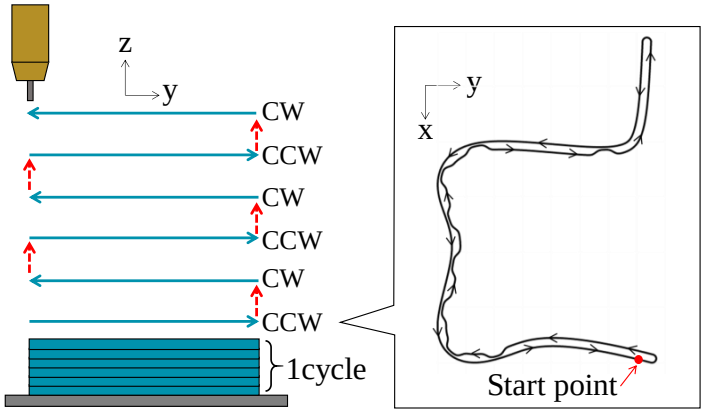

Fig.5 Torch path for deposition

Table 2 Welding parameters for deposition

Parameters	Unit	Value
Wire material	-	A5356
Wire diameter	mm	1.2
Shielding gas	-	Ar
Shielding gas flow rate	L/min	18
Current	A	120
Wire feed speed	m/min	8.1
Voltage	V	14.8
Travel speed	mm/min	1800

3.2 Result and discussion

To reach the stacking height of 420mm, 486 layers were deposited on the substrate. The height of the deposited beads tended to be higher than the surrounding area at the joints. This was because the two deposited beads slightly overlapped due to the short distance of the torch path at the joints. Therefore, the leveling process worked effectively to remove the unevenness of the build surface. In this trial, the fabrication process was stopped when the stacking height reached 420 mm to match the chair design. However, it is possible that a stacking height of more than 420 mm could have been achieved if the fabrication process had been continued.

Most of the beads at the joints were well joined to each other. However, the effective cross-sectional area of the joints was insufficient in rare cases, as shown in Figure 6. Figure 7 shows the topmost bead widths measured

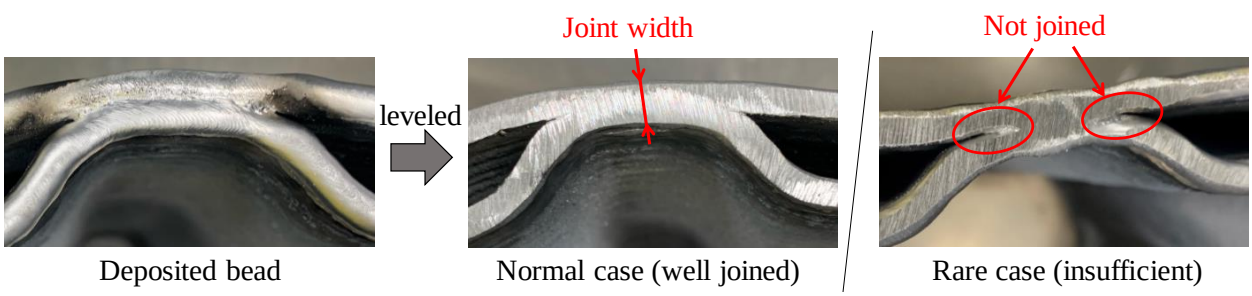

Fig.6 Joint condition

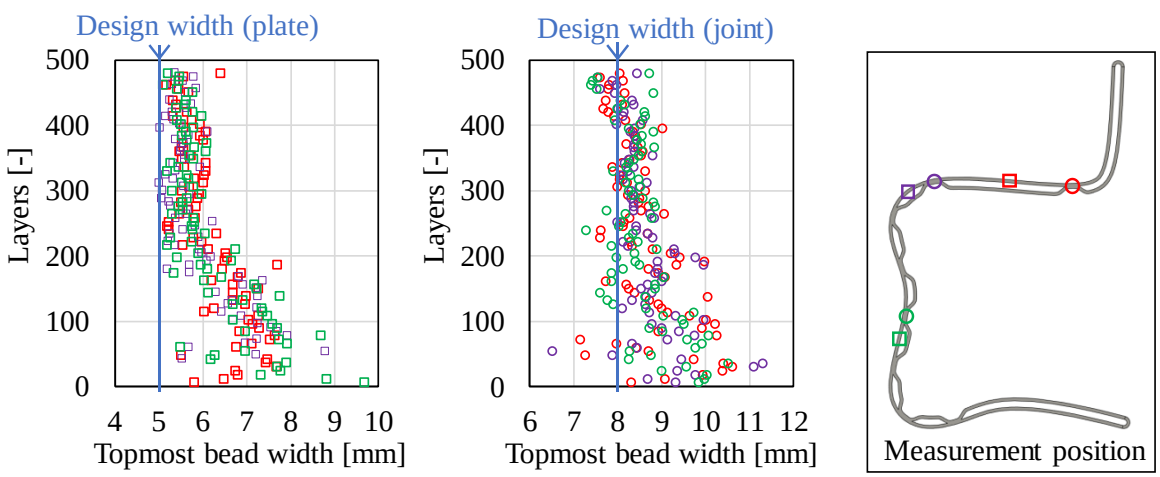

Fig.7 Topmost bead widths measured for each of the six layers deposited

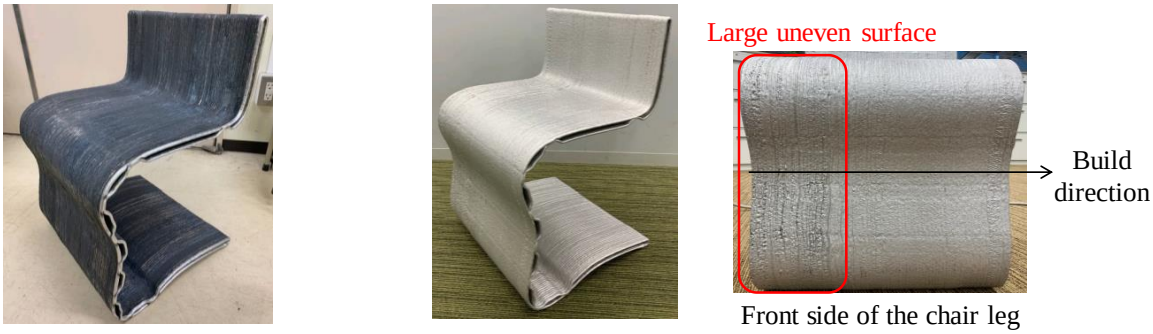

(a) Immediately after deposition (b) After surface treatment (bead blasting)

Fig. 8 Fabricated chair appearance

for each of every six layers deposited. The bead widths were wider than the designed widths and varied widely in the early layers. The average bead width at the plate was 6.7 mm (SD 0.87 mm) for layers 1-240 and 5.6 mm (SD 0.28 mm) for layers 241-486. The average bead width at the joint was 8.9 mm (SD 1.7 mm) for layers 1-240 and 8.3 mm (SD 0.34 mm) for layers 241-486. It can be presumed that the main reason for the increase and variation in bead width was the change in heat capacity during stacking. In the early layers, when the volume of the built object was small and the heat capacity was low, the temperature of the build surface may have been particularly easy to change. Consequently, the interpass temperature may have been high and varied widely, which caused the increase and variation in bead width.

Figure 8 shows the fabricated chair appearance. The black soot-like deposits were formed on the surface of the chair immediately after deposition, as shown in Figure 8(a). The reason for this is presumed that the Mg elements contained in the wire were exposed to the outside of the shielding gas, oxidized, and adhered to the surface. To remove them, the surface of the chair was treated by bead blasting after the cut-off from the substrate. The oxides were removed and the metallic luster of the aluminum was brought out by this process, as shown in Figure 8(b). However, a large unevenness was observed on the surface of the early layers due to the trial and error of the workers who performed the leveling process. This unevenness was aesthetically undesirable and needed to be resolved.

The above results showed that the method of leveling the build surface for each of the multiple layers was effective for large-sized fabrication. However, since the deposited bead widths varied widely, control of interpass temperature should be studied further to deposit beads at the designed widths. Furthermore, bead blasting was also effective in removing oxides from the aluminum surface and adjusting its appearance. The aesthetics and shape accuracy could be further improved if the manual leveling process were automated by a robot.

4. Non-destructive static loading test

4.1 Test procedure

To evaluate the structural performance, displacement and surface strain were measured while static loads were applied to the seat surface of the chair. A motion capture system was used to measure displacement, which can measure the three-dimensional movement of markers attached to the structure with an accuracy of better than 1 mm. Two digital image correlation (DIC) systems were used to measure strain, which are capable of non-contact surface measurement. Figure 9 shows the setup for the test. Seven cameras for the motion capture system and two sets of cameras for the DIC systems were installed around the chair. Spherical reflective markers were attached to the chair at a total of 12 locations, as shown in Figure 10(a), to measure the three-dimensional displacement of each marker. The measurement surfaces of the DIC systems were the front and back sides of the chair leg, as shown in Figure 10(b). Static loads were applied by placing plate-shaped weights (10kg×10) on the chair seat, as shown in Figure 10(c). The load was placed in 98.1N increments by the weights, and when it reached 981N, it was unloaded in 98.1N decrements.

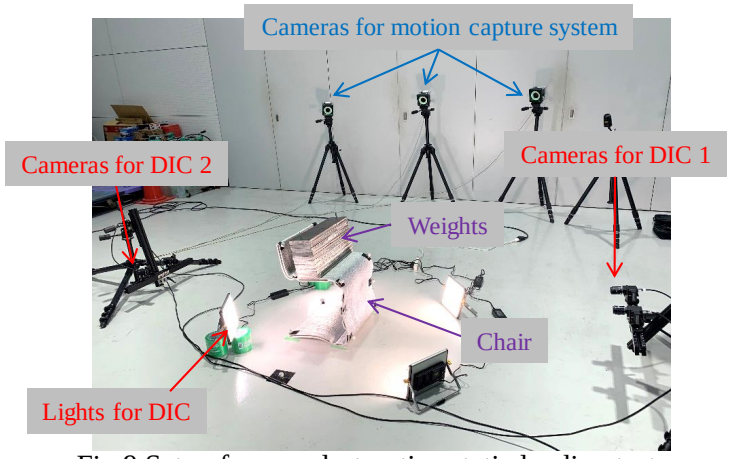

Fig.9 Setup for non-destructive static loading test

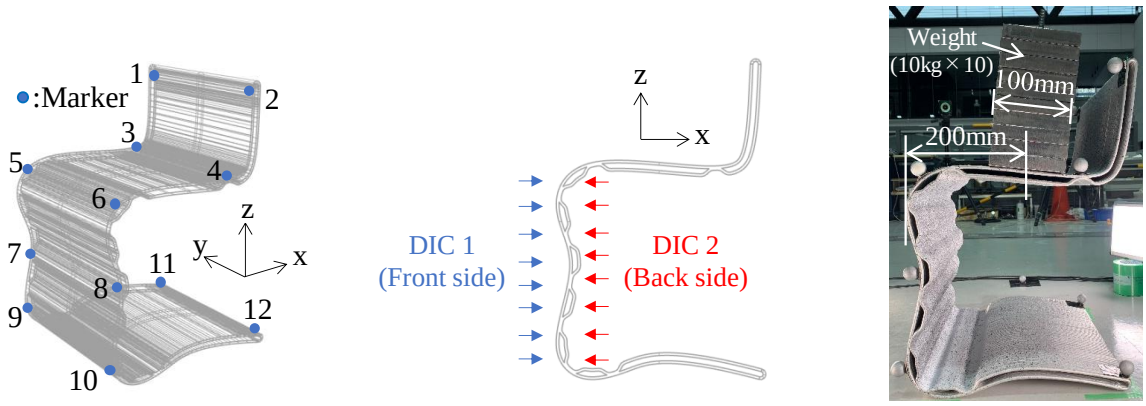

(a)Marker positions for motion capture (b) Measurement surfaces of DIC (c) Static load with weights

Fig.10 Measurement and load application method

4.2 Result and discussion

Measured values for displacement and surface strain were compared with the FEM analysis results. Figure 11 shows the displacement of Marker 1 for each load in the x- and z-directions. The displacements varied almost linearly with the loads, and the maximum absolute value of residual displacement after unloading was 0.2mm. Therefore, there was little residual displacement, and the chair was in the elastic range when the load of 981 N

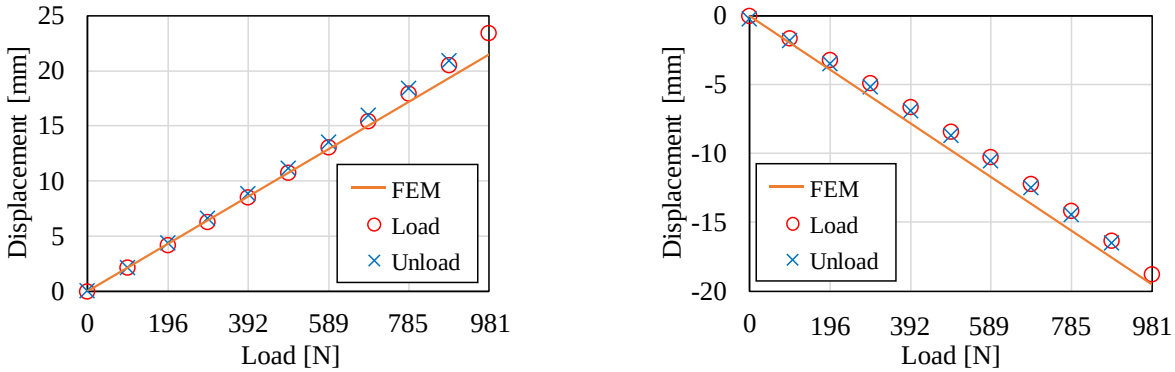

(a) x-direction (b) z-direction

Fig.11 Displacement of Marker1 for each load

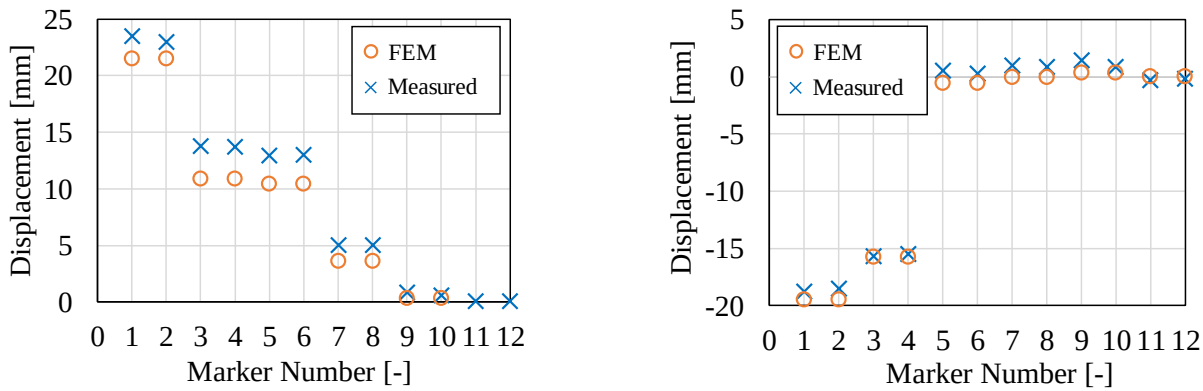

(a) x-direction (b) z-direction

Fig.12 Displacement of each marker when a load of 981N was applied

was applied, as described in Chapter 2. The absolute values of displacement in the z-direction tended to be smaller than the analytical values. This is presumably because the bead widths were wider than designed, as described in section 3.2, and thus the stiffness increased.

Figure 12 shows the displacement for each marker when a load of 981N was applied. The maximum displacement in the y-direction was 0.9 mm, which was sufficiently smaller than that in the x and z-directions, so the displacement diagram in the y-direction is omitted. In the x-direction, the maximum absolute error between the analytical and measured values was 2.88 mm at marker 3, with a relative error of 26.5%. In the z-direction, the maximum absolute error between the analytical and measured values was 0.98 mm at marker 2, with a relative error of 5.0%. In the error calculations, the analytical values were taken as true values. It can be presumed that the errors between the analytical and measured values in the large displacement region, where marker 1-6 were attached, were influenced by slight differences in force conditions. The displacements in the z-direction agreed well with the analysis because the fixation conditions of the chair were generally equal. The displacements in the x-direction deviated from the analysis compared to that in the z-direction because there were compound effects, such as the mismatch of fixing conditions of the ground contact, and the shift of the center of gravity of the load due to the inclination of the seat surface.

Figure 13 shows the contour plots of analytical and measured values of strain in the vertical direction. The minimum and maximum values of the contour plots were taken as the minimum and maximum values of the analyzed strains. In the DIC1 measurement result, large strains were concentrated near the top of the measurement area. This seems to be an incorrect measurement because this area was the boundary between the chair leg and seat, where the distance between the DIC cameras and the measured object changed abruptly. The strains were consistent with the trend of the analysis, with large absolute values at the joints. However, the absolute values of the strains were larger than the analysis partially, such as the circled area in Figure 13. It can be presumed that the insufficient cross-sectional area of the joints, mentioned in section 3.2, may have caused stress concentrations. Since only the measurement of the uppermost width was performed in the trial fabrication, the distribution of joints with insufficient cross-sectional area could not be confirmed. However, if the internal shape is revealed, the causal relationship between shape and strain will become clear.

We conclude that both displacement and strain measurements agreed well with the analytical values. Therefore, WAAM has the possibility of fabricating aluminum components with structural performance similar to that analyzed by FEM. However, since errors occurred between the analytical and measured values, it is necessary to set a safety factor to allow for this in practical use. For a more detailed study, we should establish an inspection method to obtain internal shape, which is difficult to measure after fabrication.

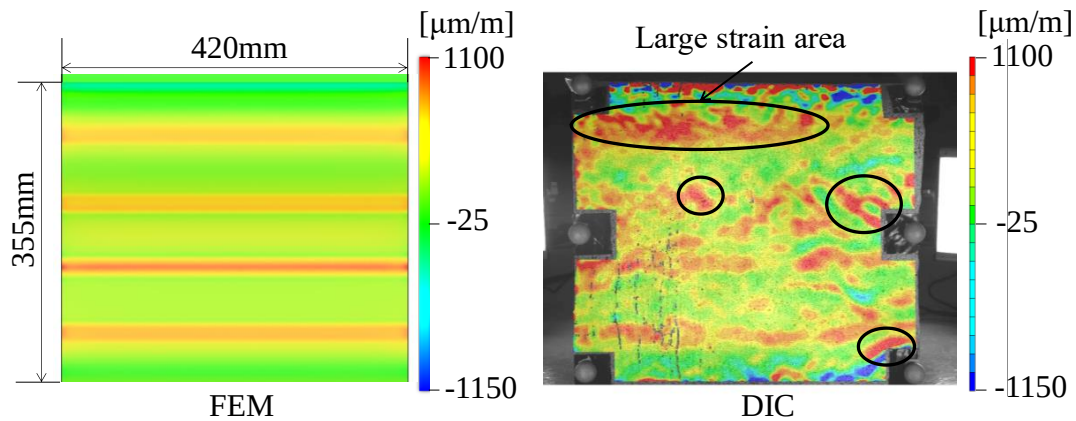

(a) Surface measured by DIC1 (Front side)

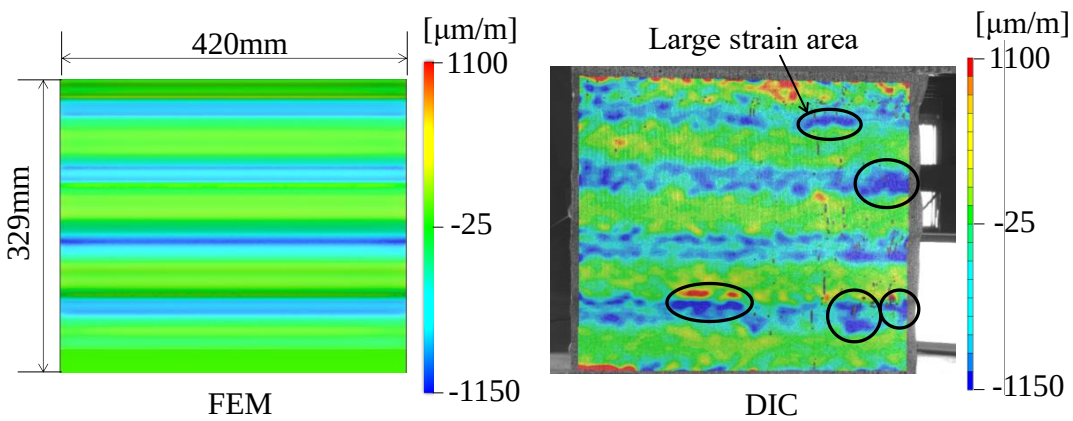

(b) Surface measured by DIC2 (Back side)

Fig.13 Contour plots of strain in the vertical direction

5. Conclusion

There are several issues in using WAAM for fabricating building facades, such as fabrication size of 4-5m, aesthetics, and structural performance. Therefore, the trial fabrication and the non-destructive static loading test were conducted to study these issues. In the study, the aluminum chair was used as a model because it contains the engineering basis of the building facades. In the trial fabrication, the method of leveling the build surface for each of the multiple layers was adopted and evaluated to investigate the possibility of large-sized fabrication. The appearance of the chair was also checked immediately after deposition and after surface treatment by bead blasting to confirm the aesthetics. In the loading test, measured displacement and strain were compared with the results of the FEM analysis to evaluate the structural performance. The results showed the followings:

(1) The method of leveling the build surface for each of the multiple layers is effective for large fabrication
(2) Bead blasting is effective in removing oxides from aluminum surfaces and adjusting their appearance
(3) WAAM has the possibility of fabricating aluminum components with structural performance similar to that analyzed by FEM

Therefore, we conclude that WAAM has the feasibility of fabricating large aluminum building facades with the structural performance expected in FEM analysis. In other words, there is a possibility to fabricate large-sized and complex-shaped building facades at a relatively low cost. Toward practical application in the construction industry, more research efforts should be conducted in the following 4 directions:

(1) Increase in fabrication size aiming for 4~5m, which is the typical height of the floor
(2) Control of interpass temperatures to improve the deposited shape accuracy
(3) Installation of a robot for leveling process to improve the aesthetics
(4) Establishment of an internal inspection method for more detailed analysis

6. References

[1] Inês Caetano, Luís Santos, António Leitão, "Computational design in architecture: Defining parametric, generative, and algorithmic design", Frontiers of Architectural Research, vol.9, pp.287-300, 2020.

[2] Carlos Bañón, Félix Raspall, "3D Printing Architecture - Workflows, Applications, and Trends", Springer, 127pp, 2021.

[3] ISO/ASTM 52900.2021, "Additive manufacturing - General principles - Fundamentals and vocabulary", 2021.

[4] Riya Singh, Akash Gupta, Ojestez Tripathi, Sashank Srivastava, Bharat Singh, Ankita Awasthi, S.K. Rajput, Pankaj Sonia, Piyush Singhal, Kuldeep K. Saxena, "Powder bed fusion process in additive manufacturing: An overview", Materials Today: Proceedings, vol.26, pp.3058-3070, 2020.

[5] C. Buchanan, L. Gardner, "Metal 3D printing in construction: A review of methods, research, applications, opportunities and challenges", Engineering Structures, vol.180, pp.332-348, 2019.

[6] Alberto Garcia-Colomo, Dudley Wood, Filomeno Martina, Stewart W. Williams, "A comparison framework to support the selection of the best additive manufacturing process for specific aerospace applications", International Journal of Rapid Manufacturing, Vol.9, pp.194-211, 2020.

[7] E. Assunção, A. Cereja, F. Martina, S. Williams, "All-in-One Machine Manufactures Large Metal Parts", pp.1-9, 2018.

[8] Leroy Gardner, Pinelopi Kyvelou, Gordon Herbert, Craig Buchanan, "Testing and initial verification of the world's first metal 3D printed bridge", Journal of Constructional Steel Research, vol.172, 2020.

[9] Jörg Lange, Thilo Feucht, Maren Erven, "3D printing with Steel - Additive Manufacturing for connections and structures", Steel Construction, vol.13, pp.144-153, 2020.

[10] BintaoWu, Zengxi Pana, Donghong Ding, Dominic Cuiuri, Huijun Li, Jing Xu, John Norrish, "A review of the wire arc additive manufacturing of metals: properties, defects and quality improvement", Journal of Manufacturing Processes, vol.35, pp.127-139, 2018.

[11] The Aluminum Association, "International Alloy Designations and Chemical Composition Limits for Wrought Aluminum and Wrought Aluminum Alloys", 2018.

[12] Y. Zhao, J. Xiao, S.J. Chen, "Comparison of Microstructure and Mechanical Properties of Aluminum Components Manufactured by CMT", Materials Science Forum, vol.898, pp.1318-1324, 2017.

[13] Markus Köhler, Jonas Hensel, Klaus Dilger, "Effects of Thermal Cycling on Wire and Arc Additive Manufacturing of Al-5356 Components", Metals, vol.10, 2020.